HHS Public Access

Author manuscript

Nanotechnology. Author manuscript; available in PMC 2017 July 15.

Published in final edited form as:

Nanotechnology. 2016 July 15; 27(28): 284002. doi:10.1088/0957-4484/27/28/284002.

3D-printed Bioanalytical Devices

Gregory W Bishop[1], **Jennifer E Satterwhite-Warden**[2], **Karteek Kadimisetty**[2], and **James F Rusling**[2,3,4,5]

[1]Department of Chemistry, East Tennessee State University, Johnson City, Tennessee 37614 [2]Department of Chemistry, University of Connecticut, Storrs, Connecticut 06269-3060 [3]Institute of Materials Science, University of Connecticut, Storrs, Connecticut 06269-3136 [4]Neag Cancer Center, University of Connecticut Health Center, Farmington, Connecticut 06030 [5]School of Chemistry, National University of Ireland at Galway, Galway, Ireland

Abstract

While 3D printing technologies first appeared in the 1980s, prohibitive costs, limited materials, and the relatively small number of commercially available printers confined applications mainly to prototyping for manufacturing purposes. As technologies, printer cost, materials, and accessibility continue to improve, 3D printing has found widespread implementation in research and development in many disciplines due to ease-of-use and relatively fast design-to-object workflow. Several 3D printing techniques have been used to prepare devices such as milli- and microfluidic flow cells for analyses of cells and biomolecules as well as interfaces that enable bioanalytical measurements using cellphones. This review focuses on preparation and applications of 3D-printed bioanalytical devices.

1. Introduction

3D printing involves the production of an object from a computer-aided design (CAD) file by depositing a material or multiple materials in successive layers using precisely controlled positioning and delivery systems. In general, 3D printing requires few steps: preparation of a design file using CAD software, generation of instructions for the printing process using a slicer program, printing the designed object by delivering or hardening a material onto a platform according to the instructions defined by the slicer program, removal of the object from the printer platform, and post-processing to remove printed supports or other extraneous material. This simple approach enables relatively rapid production of a wide variety of prototypes and offers an advantage over other fabrication methods, which usually require multiple production steps and greater capital investment in infrastructure.

Initiatives such as the RepRap and Fab@Home projects began a decade ago to promote open-source collaboration and innovation with the goal of democratizing 3D printing.[1] Consumer-grade 3D printers are now commercially available for <$1000 USD. Interest in

bishopgw@etsu.edu
james.rusling@uconn.edu

3D printing continues to grow as printers become more widely available and accessible in terms of cost and user-friendliness. Improved accessibility of 3D printers has resulted in new applications in many fields, including bioanalysis. This review is focused on the production and applications of bioanalytical devices by 3D printing.

2. 3D-printing methods

3D printing, also called additive manufacturing, can be accomplished by several strategies that vary in basic operating principles, complexity, and cost. Such techniques include deposition of thin threads of heated thermoplastic (fused deposition modeling) or viscoelastic materials (syringe deposition or direct ink writing), sintering of powders, or by exposure of photocurable resins (stereolithography) or inks (MultiJet, PolyJet) using a laser, digital light processing (DLP) projector, or other light source.[4,5] This section provides brief descriptions of some 3D printing techniques that have been employed to prepare bioanalytical devices.

2.1. Extrusion-based methods

In fused deposition modeling (FDM), a thermoplastic filament, typically 1.75 or 3.00 mm in diameter, is forced through a heated nozzle about 0.2 to 0.5 mm in diameter onto a moving platform (Figure 1). Common thermoplastic filament materials include poly(lactic acid), poly(carbonate), and acrylonitrile butadiene styrene. These materials can be purchased from commercial sources (~$30-60 USD per kg). Composite filaments that incorporate stainless steel particles, wood, ceramic powder, carbon nanotubes, and graphene are also available.

Since the layers that comprise the printed object consist of adjacent cylindrical threads of filament extruded through the heated nozzle, the surface roughness of resulting objects is often on the order of several micrometers or more,[6] which is greater than that which is possible with other 3D printing methods.[7,8] However, the simplicity of the method, compatibility with a variety of relatively inexpensive materials with different physical properties, availability of consumer-grade printers, and ability to produce objects composed of more than one material simply by including more extruder nozzles makes FDM an attractive option for prototyping and fabricating low-cost devices.

Direct ink writing, like FDM, is an extrusion-based method for producing three-dimensional objects.[9] Pioneered by Lewis et al., it involves tailoring rheological properties of colloidal suspensions and other mixtures to produce viscoelastic inks that can be deposited in layers using a pneumatically controlled syringe. Nozzle diameters as small as 1 μm have been employed to print objects from various ceramic, polymeric, and metal nanoparticle inks.[10-15]

2.2. Methods based on photopolymerization

Stereolithography (SLA) was the first form of 3D printing that was invented and commercialized.[1-5] This method employs a light source, such as a laser, to fabricate objects in a layer-by-layer fashion from photocurable resin (Figure 2). In addition to lasers, digital light processing (DLP) projectors with ultra-high-performance lamps or light emitting diodes can also be employed as sources. Printers based on DLP projectors eliminate the need for many optical components required with laser-based techniques.

Z resolution for SLA-produced objects can be submicrometer to tens of micrometers.[4] XY resolution for laser-based printing is limited by laser spot size,[16] while XY resolution for DLP-based printing is limited by pixel size. Consumer-grade DLP printers can produce objects with XY resolution of ~30-60 μm. However, printing with higher XY resolution reduces the maximum size of the object that can be printed due to the limited pixel count of DLPs.[17]

Surface roughness of objects produced by SLA can be <200 nm, and the performance of some low-cost, consumer-grade 3D-printers based on SLA can approach more expensive industrial models in terms of resolution.[18] However, parts prepared by SLA often require messy and time-consuming post-processing treatment to remove object supports and uncured resin. Due to the nature of the printing process, objects prepared by SLA are also typically limited in composition to a single epoxy or acrylate-based resin.[4]

Recently, Tumbleston et al. demonstrated that the speed of the printing process of SLA can be improved without compromising performance by incorporating an oxygen permeable window to enable continuous liquid interface production (CLIP).[19] The fundamental difference between CLIP and SLA lies in the controllable oxygen-containing layer that exists between the optical window and the cured part that is being printed. Since oxygen inhibits the photopolymerization process, a thin, controllable layer of uncured photopolymer essentially eliminates the need for steps involved in traditional SLA (exposure, replacement of resin, and movement of cured part) to be separate and discrete. Thus, CLIP reduces production times from hours to minutes by enabling object fabrication through an essentially continuous and seamless curing process.

MultiJet and PolyJet printing are similar to SLA in that they employ photocurable materials to produce objects. However, these methods rely on inkjet printing of liquid photopolymers and instant curing, typically through use of a UV lamp. MultiJet and PolyJet printers exhibit similar or better performance than SLA-based printers in terms of resolution.[4] Since multiple printer heads can be incorporated with these inkjet-based printers, MultiJet and PolyJet techniques also enable multiple material printing. However, printers based on these technologies typically cost tens of thousands to over one hundred thousand dollars or 10 to 100 times the cost of most consumer-grade 3D printers.[18]

3. 3D-printed fluidic devices

Bioanalytical measurements often require systems capable of handling small volumes (μL or less). Traditional techniques for fabricating microfluidic devices based on photolithography, milling, etching, bonding, and molding can involve cumbersome, multi-step, time-consuming processes and sometimes require large initial investments in equipment.[5,7,16,20,21] Thus, a great deal of interest has been placed on the use of 3D printing as a quick and easy alternative to traditional methods for preparing fluidic devices.

3.1. 3D-printed molds and scaffolds

3D printing was first employed to prepare master molds for poly(dimethylsiloxane) (PDMS)-based fluidics.[6] Commercially available printers based on FDM[6] and SLA,[22,23] as

well as fluorescence microscopes modified for direct laser writing (multiphoton lithography),[24,25] have been used to make molds of varying complexity. Mixing channels, channels with integrated valves, and three-dimensional fluidics that would otherwise require multiple molds and successive layer bonding have been reported.[6,22,23] Molds produced by FDM exhibit surface roughness of ~8 μm due to the nature of the printing process[6] that essentially results in an object composed of layers of adjacent thermoplastic threads, while the surface roughness of molds prepared by SLA is typically <1 μm.[22]

In addition to traditional molds, microvascular scaffolds have been demonstrated through direct-write assembly of fugitive inks.[10] Inks are deposited on a moving platform via pneumatic control of a syringe (≥10 μm dia.). Fugitive ink scaffolds can be removed from cured resin by heating to 60°C under light vacuum, ultimately resulting in microvascular networks and fluidic devices with smooth cylindrical channels (surface roughness 13.3 (± 6.5) nm) as small as 10 μm in diameter. Similarly, scaffolds for fluidic device production have also been fabricated from thermoplastic acrylonitrile butadiene styrene (ABS) via a commercially available 3D printer or 3D pen based on FDM.[26] ABS dissolves in acetone, permitting removal of the scaffold from cured PDMS to yield complex channel structures.

3.2. Directly printed devices

Fluidic devices have been directly fabricated using various 3D printing techniques. FDM of materials such as poly(propylene), poly(lactic acid), and poly(ethylene terephthalate) has resulted in the production of fluidic devices with typical limiting channel dimensions of ~500-800 μm for various applications.[27] While commercially available printers based on SLA, MultiJet, and PolyJet methods can theoretically produce channels with smaller dimensions, removal of support material from smaller channels is often difficult. Thus, limiting channel dimensions for devices prepared by these techniques are typically ~250 μm.[28,29] 500 μm high channels prepared by SLA exhibit surface roughness of ~2.54 μm,[7] while a comparison of channels fabricated using four different printers based on inkjet technology (e.g. MultiJet and PolyJet) found surface roughness to be between ~0.09 and ~2.24 μm depending on the printer.[8]

During the printing process in SLA, uncured resin becomes trapped in the channel as the top layer of the device is printed. Upon exposure of this and subsequent layers, some of the light penetrates beyond the top layer into the channel and can harden resin within the channel. Nordin et al. recently investigated the effects of optical properties of commercially available, open-source, and custom-prepared resins for SLA (DLP)-based 3D printing on minimum channel dimensions for channels printed perpendicular to the light source.[17] Resins generally consist of monomer material(s), a photoinitiator, and an absorber. The purpose of the absorber is to define the penetration depth of the incident light.

Nordin et al. found that the minimum channel height was ~3.5-5.5 times the optical penetration depth of the resin.[17] The optical penetration depth depends on the overlap of the source emission and resin absorption, and is largely controlled by absorptivity and concentration of the absorber. Custom-prepared resins composed of poly(ethylene glycol) diacrylate (PEGDA), 1% photoinitiator phenylbis(2,4,6-trimethylbenzoyl)phosphine oxide (Irgacure 819), and 0.05-0.6% absorber Sudan I exhibited penetration depths of 119 to 11

μm. Channels with minimum heights of 60 μm were prepared with 100% yield using the custom-formulated resin. Minimum channel width was found to be 4 pixels (108 μm).

Since FDM-printed devices are composed of layers of adjacent polymer threads, the overlap of threads in these layers often obscures fluids within the devices even when clear filaments are used.[30] Printing a layer of the device against a heated platform reduces surface roughness and enables adequate transparency for observation of fluids within the channels.[30] Clear photocurable resins and inks are also commercially available. However, fluidic devices printed with these materials are often opaque.[31] Post-processing by sanding with outer layers with up to 2000 grit sand paper, utilization of plastic polish, and application of a clear acrylic spray coat can be carried out to improve transparency.

3D printing enables simple and fast customization and prototyping of complex fluidic devices. For example, fluidic devices with channels that feature integrated, membrane-based pneumatically controlled valves have been directly printed by SLA.[29,32] Modular microfluidic components that can be reversibly connected using metal pins and rubber O-rings or by incorporating Lego-like interconnects in the design have been prepared using SLA and MultiJet printing.[33,34] By filling channels with fast-drying suspensions of silver particles, components like resistors and inductors for electrical circuits and wireless sensors have also been demonstrated.[35]

3.3. Bioanalytical applications of 3D-printed fluidic devices

The compositions of commercially available materials for 3D printing are usually proprietary, so it can be difficult to predict surface properties of printed objects. Internal surfaces of channels have been coated with materials that feature desired functional groups to alter surface characteristics. For example, layers of PDMS or poly(styrene) were deposited on the internal surfaces of PolyJet-printed fluidic channels to promote cellular adhesion for electrically-promoted lysis experiments.[31] After 5 days, 94-98% of cells adhered to the modified channels survived, and lysis efficiency was ~95% for applied electric field strengths ≥250 V cm^{-1}.

Spence et al. showed that a PolyJet printer can be used to fabricate fluidic devices that feature threaded ports to allow convenient access to channels.[36] These ports provide interfaces for commercially available fittings and allow integration of membrane inserts[36,p37] and electrodes for bioanalytical applications.[31,38] Membrane inserts are commonly used in cell culture studies and serve to selectively transport small molecules from the channel where cells are present to a reservoir where measurements can be made. Effects of saponin on cell viability and storage conditions on the ability of red blood cells to produce adenosine triphosphate (ATP) were studied using 3D-printed fluidic devices that featured removable membrane inserts.[36,37] In some studies, fluidic devices were designed so that the positions of membrane inserts and measurement reservoirs enabled analyses to be performed by a commercial plate reader (Figure 3).[37]

Measurement devices can be integrated into threaded fittings for reversible inclusion into 3D-printed channels or may be fixed into access holes using epoxy. Optical fibers have been incorporated for simple UV-Vis absorption measurements of fluids.[8] Detection of dopamine,

nitric oxide, and adenosine triphosphate (ATP) in 500 μm × 500 μm channels has been accomplished using an integrated 1 mm glassy carbon rod or 250 μm platinum black wire electrode.[38] Oxygen was electrochemically detected in a flowing sample of red blood cells (RBCs), and ATP released by RBCs was collected by membrane inserts located downstream from the electrodes, where it could be measured by chemiluminescence. RBCs with low oxygen levels (4.8 (±0.5) ppm) produced 2.4 (±0.4) times more ATP than RBCs with normal oxygen levels (8.2 (±0.6) ppm).

Continuous monitoring of glucose and lactate in human tissues has also been demonstrated by interfacing 3D-printed fluidic devices that feature integrated needle electrode biosensors with an FDA-approved clinical microdialysis probe.[39] Microdialysis probes were inserted into human subjects, and small, wearable fluidic devices were designed so dialysate from the probe flowed past needle electrode biosensors. Levels of glucose and lactate were monitored as the subjects performed exercise in the form of cycling and during a post-workout resting period. Glucose level in the dialysate decreased from an initial value of 6 (±1) mM to 1.84 (±0.05) mM, while lactate level was found to be 1.8 (±0.3) mM initially 1.67 (±0.3) mM after the resting period.

3-sided SLA-printed channels have been interfaced with electrodes deposited on Si/SiO_2 or embedded in epoxy by fastening the electrode substrate and open face of the channel together using thread.[40] Virus particles labeled with CdS quantum dots have been detected by differential pulse voltammetry of Cd^{2+} using electrodes incorporated in FDM-printed channels.[41] Integration of electrodes through threaded ports has also been demonstrated using low-cost, consumer-grade FDM and SLA. Due to the limited resolution of consumer grade FDM printers, threaded ports were custom-designed with wider threads to incorporate electrodes coated with films of Prussian blue nanoparticles for detection of H_2O_2.[30] Good optical transparency of SLA-printed fluidic devices enabled measurement of electrochemiluminescence (ECL) from tris(2,2'-bipyridyl)ruthenium (II) ($Ru(bpy)_3^{2+}$) aided by tri-*n*-propylamine or guanine bases of DNA using 0.5 mm graphite electrodes.[42]

4. 3D-printed interfaces and prototypes for bioanalysis

Low-cost, easy-to-use, portable, energy-efficient bioanalytical instrumentation is necessary for improving care in resource-limited settings where laboratory infrastructure is inaccessible. Such characteristics are also essential for point-of-care analyses where immediate measurement and interpretation of results is required. As a result, recent interest has centered on using 3D printing to fabricate prototypes and interfaces that enable automated or semi-automated bioanalytical measurements.

An FDM-printed gravity flow delivery system for performing multi-step electrochemiluminescence-based sandwich immunoassays has been reported (Figure 4).[43] The system consists of reservoirs for holding reagents and wash buffers that can be delivered to a screen-printed carbon electrode array adhered to the bottom of a 3D-printed open-channel flow cell. Once delivered, reagents are held on the surface of the electrodes for defined incubation periods necessary for the assay.

After incubation periods, reagents are removed from the surface by gravity flow initiated by moving an adjustable platform controlled by a lever that is used to change the resting angle of the flow cell. Wash buffers are then delivered to the flow cell to remove unbound reagents and other potential interferents. Using this setup, a multiplex ECL-based assay was performed for prostate cancer biomarkers: prostate specific antigen (PSA), prostate specific membrane antigen (PSMA), and platelet factor-4 (PF-4).

Electrodes were modified with antibodies, and the 3D-printed delivery system was used to introduce serum samples (2-5 μL), protein labels (silica nanoparticles loaded with ECL dye $Ru(bpy)_3^{2+}$ and surface-modified with biomarker-specific antibodies), and wash buffers to the electrode array. A bioimaging system equipped with a charge-coupled device camera is used to obtain ECL signal. Multiplex assay results compared favorably to traditional enzyme-linked immunosorbent assays.

The relatively low-cost and ease-of-operation offered by 3D printing has been especially attractive for researchers developing hardware for cellphone-based bioanalytical instruments. The Ozcan group has successfully employed 3D printing to create mechanical interfaces that permit cellphones to serve as instruments for a variety of bioanalyses. A colorimetric assay for peanut allergen was demonstrated through the use of 3D printing to fabricate a sample holder and positioning system that enables placement of glass tubes containing analyte and light-emitting diodes (LEDs) in front of the cellphone camera (Figure 5).[44]

A commercially available food allergen testing kit was used to convert peanut allergen into a measurable colorimetric signal. LEDs (650 nm peak wavelength with 15 nm bandwidth) were used to illuminate samples and control vials to enable absorption-based measurement of the allergen test kit substrate via the cellphone camera. A custom cellphone application was developed for capturing and processing images to determine peanut allergen concentrations of 1-25 ppm. Cellphone-based colorimetric detection of mercury from water samples using a similar strategy has also been reported.[45]

A portable microplate reader has been demonstrated by incorporating 96 optical fibers and 24 LEDs in a 3D-printed cellphone interface.[46] The microplate reader was used to analyze over 500 patient samples for mumps, measles, and herpes simplex virus (HSV) IgGs in a clinical microbiology laboratory setting using colorimetric enzyme-linked immunosorbent assays. Fast, remote analyses of the collected data were performed using a custom-designed app that delivered results to the researchers' servers within ~1 min per 96-well plate. Accuracies >99% were reported for mumps, HSV-1, and HSV-2 tests, while the accuracy for the measles test was 98.6%.

Assays for cholesterol in human serum and saliva as well as lactate in artificial saliva and sweat have been conducted with the aid of FDM-printed devices that enable cellphone-based chemiluminescence measurements.[47,48] A 3D-printed adaptor was used to interface the phone with a 3D-printed cartridge that contained necessary reagents for enzyme-catalyzed chemiluminescence reactions. Cholesterol oxidase, cholesterol esterase, horseradish peroxidase, and L-lactate oxidase were immobilized on nitrocellulose membranes inserted in

the cartridges. Detection was based on luminescence provided by the reaction of luminol and hydrogen peroxide generated from the reaction of oxidase enzyme with the analyte.

Fluorescence-based assays and measurements performed using cellphones with 3D-printed hardware interfaces have also been demonstrated.[49-51] These devices include housing for a battery-powered diode laser positioned perpendicular with respect to the camera lens and an interference filter placed in front of the camera for emission measurements. The detection limit for albumin in urine using a fluorescence-based assay completed using a cellphone was reported to be 5-10 μM, >3 times smaller than the normal range.[49]

The simplicity and speed of 3D printing, ubiquity of cellphones, and fluorescence-based measurements have helped make nanoscale imaging more accessible.[52] Cellphone-based fluorescence microscopes with 3D-printed components have recently been demonstrated for imaging of single 100-nm-diameter particles and fluorescently-labeled viruses.[50] Sizing of single DNA molecules has also been recently reported.[51]

5. Conclusions

Limited resource settings and the immediacy required in some circumstances present special challenges for bioanalytical measurements. Devices capable of addressing these challenges should be low in cost and easy to use while consuming little power. Thus, the simple and fast design-to-object workflow offered by 3D printing has been especially attractive for the fabrication of bioanalytical devices.

Milli- and microfluidic devices required to handle limited volumes of biological materials have been prepared from molds and scaffolds as well as direct printing. Optical and electrochemical methods have been employed for measurements of proteins and enzyme reaction products in 3D-printed fluidic devices.

3D-printed devices for interfacing cellphones with LEDs, laser diodes, filters, and lenses have resulted in fluorescence and colorimetric-based assays for allergens, proteins, nucleic acids, and nanoparticles. Cellphone-based microscopes have been described for nanoscale fluorescence imaging. Microplate readers have resulted from the integration of optical fibers in a 3D-printed measurement interface. 3D printing technologies are capable of hastening the pace of innovation by democratizing device production processes through their simple and fast design-to-object capabilities.

6. Acknowledgements

This work was supported financially by grants Nos. EB016707 and EB14586 from the National Institute of Biomedical Imagining and Bioengineering (NIBIB), NIH.

References

1. Ventola CL. Medical applications for 3D printing: current and projected uses. Pharmacol. Ther. 2014; 39:704–11.
2. [May 22, 2015] 3D printer schematic is based on MakerBot Replicator Dual Model by colec18. published June 24, 2014 http://www.thingiverse.com/thing:372804

3. [November 10, 2015] Illustrated drive gear is based on Extruder gear wheel (rueda dentada) by dracnas. published January 19, 2015 http://www.thingiverse.com/thing:642331
4. Gross BC, Erkal JL, Lockwood SY, Chen C, Spence DM. Evaluation of 3D printing and its potential impact on biotechnology and the chemical sciences. Anal. Chem. 2014; 86:3240–53. [PubMed: 24432804]
5. O'Neill PF, Azouz AB, Vázquez M, Liu J, Marczak S, Slouka Z, Chang HC, Diamond D, Brabazon D. Advances in three-dimensional rapid prototyping of microfluidic devices for biological applications. 8. Biomicrofluidics. 2014:052112.
6. McDonald JC, Chabinyc ML, Metallo SJ, Anderson JR, Stroock AD, Whitesides GM. Prototyping of microfluidic devices in poly(dimethylsiloxane) using solid-object printing. Anal. Chem. 2002; 74:1537–45. [PubMed: 12033242]
7. Au AK, Lee W, Folch A. Mail-order microfluidics: evaluation of stereolithography for the production of microfluidic devices. Lab Chip. 2014; 14:1294–1301. [PubMed: 24510161]
8. Walczak R, Adamski K. Inkjet 3D printing of microfluidic structures—on the selection of the printer towards printing your own microfluidic chips. J. Micromech. Microeng. 2015; 25:085013.
9. Lewis JA. Direct ink writing of 3D functional materials. Adv. Funct. Mater. 2006; 16:193–204.
10. Therriault D, White S, Lewis JA. Chaotic mixing in three-dimensional microvascular networks fabricated by direct-write assembly. Nat. Mater. 2003; 2:265–71. [PubMed: 12690401]
11. Ahn BY, Duoss EB, Motala MJ, Guo X, Park S-I, Xiong Y, Yoon J, Nuzzo RG, Rogers JA, Lewis JA. Omnidirectional printing of flexible, stretchable, and spanning silver microelectrodes. Science. 2009; 323:1590–1593. [PubMed: 19213878]
12. Wu W, DeConinck A, Lewis JA. Omnidirectional printing of 3D microvascular networks. Adv. Mater. 2011; 23:H178–83. [PubMed: 21438034]
13. Sun K, Wei T-S, Ahn BY, Seo JY, Dillon SJ, Lewis JA. 3D printing of interdigitated Li-ion microbattery architectures. Adv. Mater. 2013; 25:4539–43. [PubMed: 23776158]
14. Compton BG, Lewis JA. 3D-printing of lightweight cellular composites. Adv. Mater. 2014; 26:5930–5. [PubMed: 24942232]
15. Muth JT, Vogt DM, Truby RL, Mengüç Y, Kolesky DB, Wood RJ, Lewis JA. Embedded 3D printing of strain sensors within highly stretchable elastomers. Adv. Mater. 2014; 26:6307–12. [PubMed: 24934143]
16. Ho C MB, Ng SH, Li KHH. 3D printed microfluidics for biological applications. Lab Chip. 2015; 15:3627–37. [PubMed: 26237523]
17. Gong H, Beauchamp M, Perry S, Woolley AT, Nordin GP. Optical approach for resin formulation for 3D printed microfluidics. RSC Adv. 2015; 5:106621–32. [PubMed: 26744624]
18. Comina G, Suska A, Filippini D. Low cost lab-on-a-chip prototyping with a consumer grade 3D printer. Lab Chip. 2014; 14:2978–82. [PubMed: 24931176]
19. Tumbleston JR, Shirvanyants D, Ermoshkin N, Janusziewicz R, Johnson AR, Kelly D, Chen K, Pinschmidt R, Rolland JP, Ermoshkin A, Samulski ET, DeSimone JM. Science. 2015; 347:1349–52. [PubMed: 25780246]
20. Waldbaur A, Rapp H, Länge K, Rapp BE. Let there be chip–towards rapid prototyping of microfluidic devices: one-step manufacturing processes. Anal. Methods. 2011; 3:2681–716.
21. Nge PM, Rogers CI, Woolley AT. Advances in microfluidic materials, functions, integration, and applications. Chem. Rev. 2013; 113:2550–83. [PubMed: 23410114]
22. Comina G, Suska A, Filippini D. PDMS lab-on-a chip fabrication using 3D printed templates. Lab Chip. 2014; 14:424–30. [PubMed: 24281262]
23. Chan HN, Chen Y, Shu Y, Chen Y, Tian Q, Wu H. Direct, one-step molding of 3D-printed structures for convenient fabrication of truly 3D PDMS microfluidic chips Microfluid. Nanofluid. 2015; 19:9–18.
24. Spivey EC, Xhemalce B, Shear JB, Finkelstein IJ. 3D-printed microfluidic microdissector for high-throughput studies of cellular aging. Anal. Chem. 2014; 86:7406–12. [PubMed: 24992972]
25. LaFratta CN, Simoska O, Pelse I, Weng S, Ingram M. A convenient direct laser writing system for the creation of microfluidic masters. Microfluid. Nanofluid. 2015; 19:419–26.

26. Saggiomo V, Velders AH. Simple 3D printed scaffold-removal method for the fabrication of intricate microfluidic devices. Adv. Sci. 2015; 2:1500125.
27. Kitson PJ, Rosnes MH, Sans V, Dragone V, Cronin L. Configurable 3D-Printed millifluidic and microfluidic 'lab on a chip' reactionware devices. Lab Chip. 2012; 12:3267–71. [PubMed: 22875258]
28. Shallan AI, Smejkal P, Corban M, Guijt RM, Breadmore MC. Cost-effective three-dimensional printing of visibly transparent microchips within minutes. Anal. Chem. 2014; 86:3124–30. [PubMed: 24512498]
29. Rogers CI, Qaderi K, Woolley AT, Nordin GP. 3D printed microfluidic devices with integrated valves. Biomicrofluidics. 2015; 9:016501. [PubMed: 25610517]
30. Bishop GW, Satterwhite JE, Bhakta S, Kadimisetty K, Gillette KM, Rusling JF. 3D-printed fluidic devices for nanoparticle preparation and flow-injection amperometry using integrated Prussian blue nanoparticle-modified electrodes. Anal. Chem. 2015; 87:5437–43. [PubMed: 25901660]
31. Gross BC, Anderson KB, Meisel JE, McNitt MI, Spence DM. Polymer coatings in 3D-printed fluidic device channels for improved cellular adherence prior to electrical lysis. Anal. Chem. 2015; 87:6335–41. [PubMed: 25973637]
32. Au AK, Bhattacharjee N, Horowitz LF, Chang TC, Folch A. 3D-printed microfluidic automation. Lab Chip. 2015; 15:1934–41. [PubMed: 25738695]
33. Lee KG, Park KJ, Seok S, Shin S, Kim DH, Park JY, Heo YS, Lee SJ, Lee TJ. 3D printed modules for integrated microfluidic devices. RSC Adv. 2014; 4:32876–80.
34. Bhargava KC, Thompson B, Malmstadt N. Discrete elements for 3D microfluidics. Proc. Natl. Acad. Sci. 2014; 111:15013–8. [PubMed: 25246553]
35. Wu S-Y, Yang C, Hsu W, Lin L. 3D-printed microelectronics for integrated circuitry and passive wireless sensors. Microsys. & Nanoeng. 2015; 1:15013.
36. Anderson KB, Lockwood SY, Martin RS, Spence DM. A 3D printed fluidic device that enables integrated features. Anal. Chem. 2013; 85:5622–6. [PubMed: 23687961]
37. Chen C, Wang Y, Lockwood SY, Spence DM. 3D-printed fluidic devices enable quantitative evaluation of blood components in modified storage solutions for use in transfusion medicine. Analyst. 2014; 139:3219–26. [PubMed: 24660218]
38. Erkal JL, Selimovic A, Gross BC, Lockwood SY, Walton EL, McNamara S, Martin RS, Spence DM. 3D printed microfluidic devices with integrated versatile and reusable electrodes. Lab Chip. 2014; 14:2023–32. [PubMed: 24763966]
39. Gowers SAN, Curto VF, Seneci CA, Vadgama P, Yang G-Z, Boutelle MG. 3D printed microfluidic device with integrated biosensors for analysis of subcutaneous human microdialysate. Anal. Chem. 2015; 87:7763–70. [PubMed: 26070023]
40. Snowden ME, King PH, Covington JA, Macpherson J, Unwin PR. Fabrication of Versatile Channel Flow Cells for Quantitative Electroanalysis Using Prototyping. Anal. Chem. 2010; 82:3124–31. [PubMed: 20329754]
41. Krejcova L, Nejdl L, Rodrigo M AM, Zurek M, Matousek M, Hynek D, Zitka O, Kopel P, Adam V, Kizek R. 3D printed chip for electrochemical detection of influenza virus labelled with CdS quantum dots Biosens. Bioelectron. 2014; 54:421–7.
42. Bishop GW, Satterwhite-Warden JE, Bist I, Chen E, Rusling JF. Electrochemiluminescence at bare and DNA-coated graphite electrodes in 3D-printed fluidic devices. ACS Sensors. 2016; 1:197–202. [PubMed: 27135052]
43. Kadimisetty K, Mosa IM, Malla S, Satterwhite-Warden JE, Kuhns TM, Faria RC, Lee NH, Rusling JF. 3D-printed supercapacitor-powered electrochemiluminescent protein immunoarray. Biosens. Bioelectron. 2016; 77:188–93. [PubMed: 26406460]
44. Coskun AF, Wong J, Khodadadi D, Nagi R, Tey A, Ozcan A. A personalized food allergen testing platform on a cellphone. Lab Chip. 2013; 13:636–40. [PubMed: 23254910]
45. Wei Q, Nagi R, Sadeghi K, Feng S, Yan E, Ki SJ, Caire R, Tseng D, Ozcan A. Detection and spatial mapping of mercury contamination in water samples using a smart-phone. ACS Nano. 2014; 8:1121–9. [PubMed: 24437470]
46. Berg B, Cortazar B, Tseng D, Ozkan H, Feng S, Wei Q, Chan RY-L, Burbano J, Farooqui Q, Lewinski M, Di Carlo D, Garner OB, Ozcan A. Cellphone-based hand-held microplate reader for

point-of-care testing of enzyme-linked immunosorbent assays. ACS Nano. 2015; 8:7857–66. [PubMed: 26159546]

47. Roda A, Michelini E, Cevenini L, Calabria D, Calabretta MM, Simoni P. Integrating biochemiluminescence detection on smartphones: mobile chemistry platform for point-of-need analysis. Anal. Chem. 2014; 86:7299–304. [PubMed: 25017302]
48. Roda A, Guardigli M, Calabria D, Calabretta MM, Cevenini L, Michelini E. A 3D-printed device for a smartphone-based chemiluminescence biosensor for lactate in oral fluid and sweat. Analyst. 2014; 139:6494–501. [PubMed: 25343380]
49. Coskun AF, Nagi R, Sadeghi K, Phillips S, Ozcan A. Albumin testing in urine using a smart-phone. Lab Chip. 2013; 13:4231–8. [PubMed: 23995895]
50. Wei Q, Qi H, Luo W, Tseng D, Ki SJ, Wan Z, Göröcs, Bentolila LA, Wu T-T, Sun R, Ozcan A. Fluorescent imaging of single nanoparticles and viruses on a smart phone. ACS Nano. 2013; 7:9147–55. [PubMed: 24016065]
51. Wei Q, Luo W, Chiang S, Kappel T, Mejia C, Tseng D, Chan RYL, Qi H, Shabbir F, Ozkan H, Feng S, Ozcan A. Imaging and sizing of single DNA molecules on a mobile phone. ACS Nano. 2014; 8:12725–33. [PubMed: 25494442]
52. McLeod E, Wei Q, Ozcan A. Democratization of nanoscale imaging and sensing tools using photonics. Anal. Chem. 2015; 87:6434–45. [PubMed: 26068279]

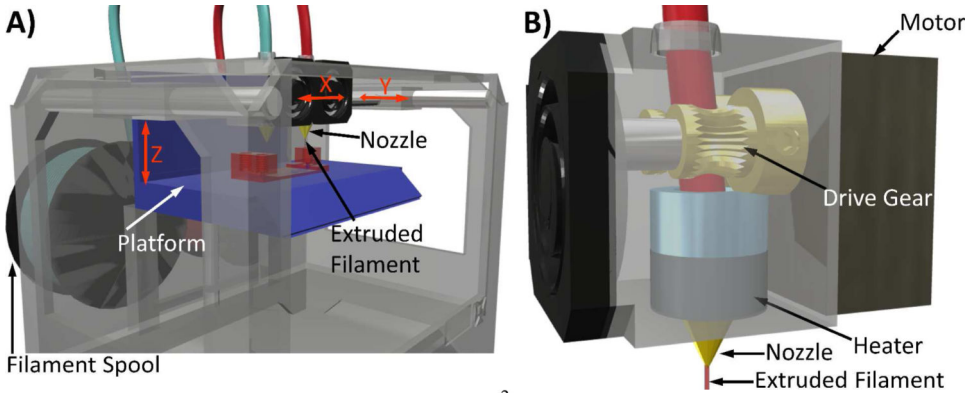

Figure 1.

Illustrated schematic of an FDM 3D printer.[2] A) Thermoplastic filament is fed through a heated nozzle onto a moving platform. A gantry system controls X and Y movements of the extruder assembly. B) Components of the extruder assembly are depicted. Drive gear[3] and motor used to deliver filament to heated nozzle.

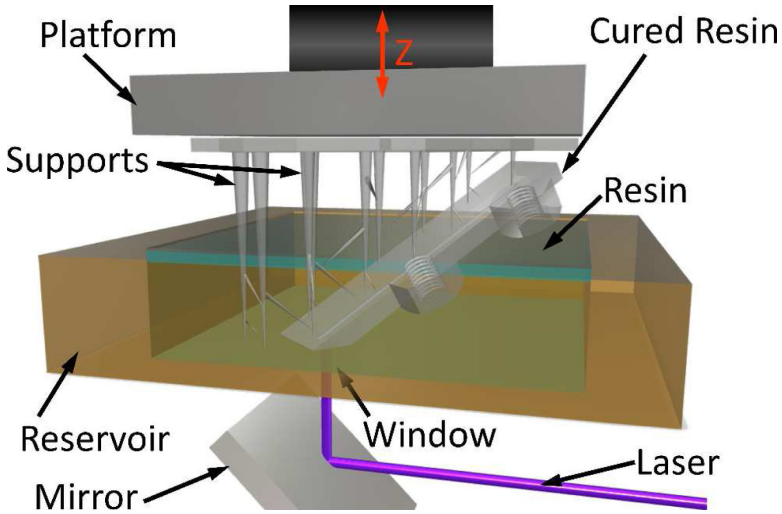

Figure 2.
Illustrated schematic of a laser-based SLA 3D printer.

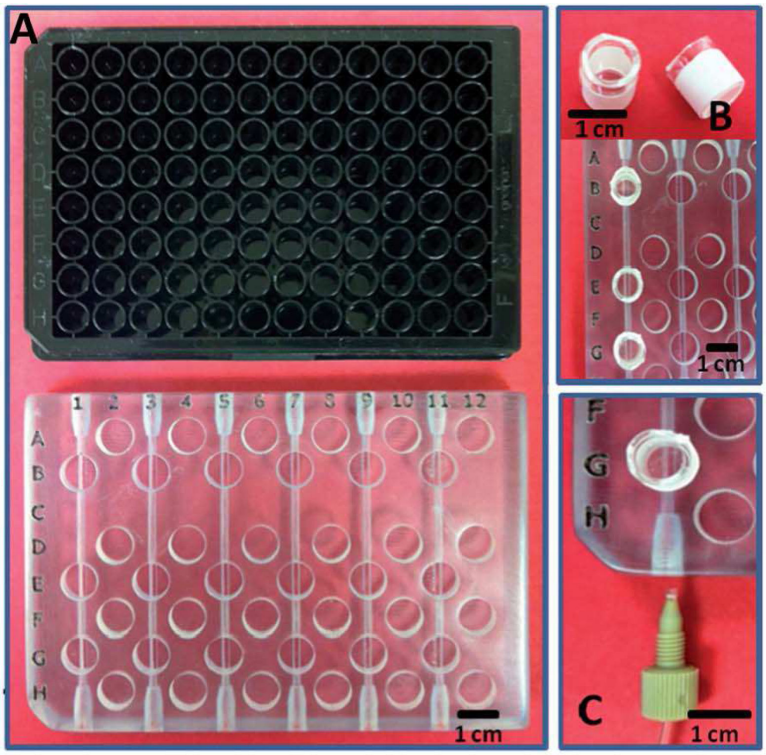

Figure 3.

Images of a 3D-printed fluidic device for determination of adenosine triphosphate released by erythrocytes. A) The design for the fluidic device (bottom) was based on a 96-well plate (top) so that a commercial plate reader could be used for measurements. B) Membrane inserts (top) were placed in the printed wells (bottom, leftmost channel). C) Fluidic channels were connected to fluid delivery system (pump) via commercially available fittings and tubing. Adapted from Reference 37 with permission from the Royal Society of Chemistry.

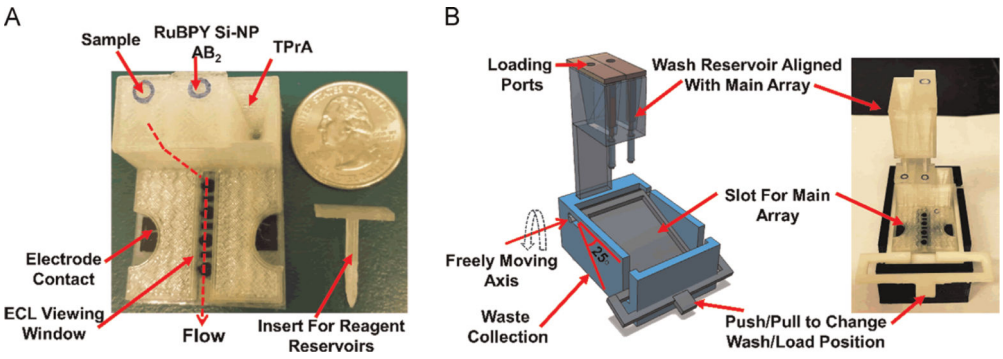

Figure 4.

FDM-printed devices that enable gravity-flow reagent and washing buffer delivery for ECL-based immunoassays. (A) A screen-printed electrode array is affixed to the bottom of a 3D-printed reagent delivery system. Serum sample, antibody (AB_2)-labeled silica nanoparticles (Si-NP) filled with ECL dye $Ru(bpy)_3^{2+}$, and ECL coreactant tri-*n*-propylamine are stored in reservoirs. Delivery of reagents to the open-top channel is accomplished by removing reservoir inserts. B) 3D model (left) and photograph of wash reservoir module showing freely moving lever to change between wash and load positions. A lever is used to adjust the position of the array so that reagents or washing buffer can be held on the electrode array surface for incubation or flowed over for washing. Reprinted from Reference 43 with permission from Elsevier.

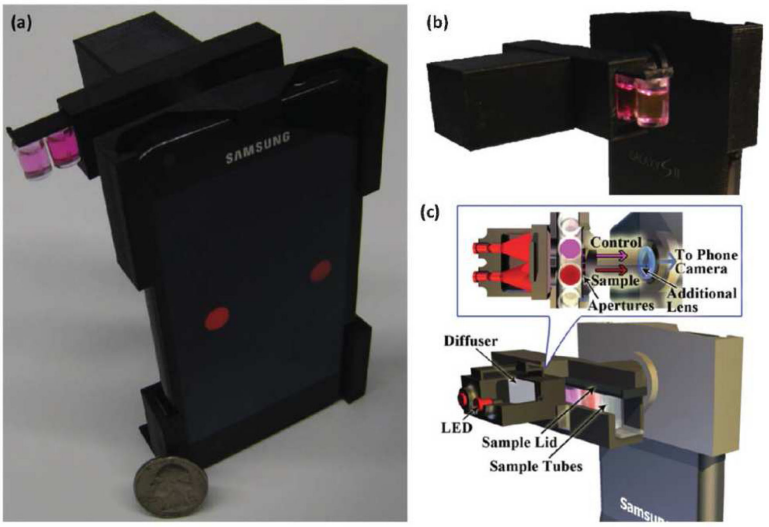

Figure 5.

Cellphone-based colorimetric assay for peanut allergen conducted using a 3D-printed platform for sample handling. (a) A photograph of 3D-printed platform is connected to a smartphone for sample measurement. (b) An opto-mechanical attachment (dimensions: ~22 mm × 67 mm × 75 mm) equipped with light-emitting diodes enables colorimetric measurements by the cellphone camera. (c) A schematic diagram of the interface, depicting components of the opto-mechanical attachment. Reproduced from Reference 44 with permission of The Royal Society of Chemistry.